Abdominal Radiology

Published online: 15 October 2018

Abdom Radiol (2019) 44:1062–1069
https://doi.org/10.1007/s00261-018-1804-9

Prostate MRI using an external phased array wearable pelvic coil at 3T: comparison with an endorectal coil

Rory L. O'Donohoe,[1] Ruth M. Dunne,[1] Vera Kimbrell,[1] and Clare M. Tempany[1]

[1]Department of Radiology, Brigham and Women's Hospital, 75 Francis St, Boston, MA 02115, USA

Abstract

Purpose: To evaluate T2w and DWI image quality using a wearable pelvic coil (WPC) compared with an endorectal coil (ERC).

Methods: Twenty men consecutively presenting to our prostate cancer MRI clinic were prospectively consented to be scanned using a wearable pelvic coil then an endorectal coil and pelvic phased array coil at 3T. Eighteen patients were suitable for inclusion. Axial T2w images were obtained using the WPC and ERC, and DWI images were obtained using the WPC, ERC, and PPA. Analysis was performed in consensus by two readers with experience in prostate MRI. The readers scored the T2w images using six qualitative criteria and the DWI images using five criteria. Signal-to-noise ratio (SNR) was also measured.

Results: T2w artifact severity was greater for an ERC than a WPC ($p = 0.003$). There was no significant difference in T2w qualititatve image quality by other measures. The distinction of zonal anatomy on DWI was superior for an ERC compared with both a WPC and a PPA ($p = 0.018$ and $p < 0.001$ respectively), and there was no significant difference in DWI image quality by other measures. SNR was significantly higher for ERC imaging for both T2w and DWI.

Conclusion: WPC imaging provides comparable image quality to that of an ERC, potentially reducing the need for an ERC. WPC imaging shows reduced T2w artifact severity and inferior DWI zonal anatomy distinction compared with an ERC. Imaging with a WPC produces a lower SNR than an ERC.

Key words: Prostate—MRI—Endorectal coil—Wearable pelvic coil

Correspondence to: Rory L. O'Donohoe; *email:* rory.odonohoe@tuh.ie

The role of multiparametric magnetic resonance imaging (mpMRI) of the prostate has grown to be central in the management of prostate cancer. It is used in the local staging of prostate cancer [1, 2], can provide information about tumor aggressiveness [3–5], allows lesion localization for targeted biopsy [6, 7] and can be used as part of an active surveillance program [8]. In addition to this, there is developing evidence that mpMRI can be used in the initial workup of patients in whom prostate cancer is suspected based on the elevation of serum prostate specific antigen (PSA) or findings on digital rectal examination [9].

As the importance of prostate mpMRI increases, so does the need to optimize methods for image acquisition. At present, mpMRI examinations are typically performed at 1.5T or 3T using a pelvic phased array coil (PPA) with or without the addition of an endorectal coil (ERC) to increase the signal-to-noise ratio (SNR). The precise imaging technique that is used varies across institutions. In the Prostate Imaging—Reporting and Data System version 2 (PI-RADS v2) published in 2015, the authors note that credible imaging results have been obtained without an ERC at 1.5T and 3T, but the combination of a PPA and ERC increases the SNR at any field strength, and with some 1.5T systems the use of an ERC is indispensible [10].

After factoring in issues of time, cost, and patient acceptability, there is currently no consensus on the optimal imaging technique. A number of studies have been performed comparing image quality using different field strengths and coil configurations. A recent prostate mpMRI study comparing the image quality obtained at 3T using a PPA and a PPA/ERC combination found that T2-weighted (T2w) images were of comparable quality and that diffusion-weighted images (DWI) obtained with an ERC demonstrated superior image quality for one of two readers [11]. The same study found a higher SNR for DWI using a PPA over a PPA/ERC combination, and no significant difference in SNR was found between the two

for T2w. Another study comparing the diagnostic utility of ERC and non-ERC mpMRI at 3T found ERC examinations to be superior at detecting cancer foci [12].

Since prostate mpMRI involves the acquisition of signal from a small volume of tissue, positioning the receive coil as near as possible to the gland may be advantageous. A new wearable pelvic coil aims to optimize non-ERC mpMRI by positioning the coil elements as close as possible to the perineum and therefore the prostate gland. By physically wrapping around and conforming to the pelvis, the coil aims to maximize the signal obtained from the prostate gland. The purpose of this study is to compare the qualitative and quantitative image quality of T2w and diffusion-weighted images acquired using a wearable pelvic coil and an endorectal coil.

Materials and methods

Approval was obtained from the institutional ethical review board, and the study is compliant with the Health Insurance Portability and Accountability Act. Written informed consent was obtained from all individual participants included in the study.

Patients

Twenty men presenting to our prostate cancer MRI clinic as part of a diagnostic workup were prospectively consented to be scanned using an external phased array wearable pelvic coil (WPC) in addition to the standard diagnostic sequences obtained using a endorectal coil (ERC) and standard pelvic phased array coil (PPA) at 3T. All patients were presenting for the assessment of known or suspected prostate cancer. Two patients were excluded, one of whom did not tolerate ERC insertion and the other having undergone prior prostatectomy. Eighteen patients were included in the study. The age range was 49–72 (mean 63) and the prostate-specific antigen (PSA) range was 2.0–87.0 (mean 10.0). A PSA level was unavailable for one patient, having been measured at an outside institution.

MRI technique

All imaging was performed on the same 3T MR system (Discovery MR750w, GE Healthcare, Waukesha WI, USA). The wearable pelvic coil (PROCURE Prostate/Pelvic Coil, ScanMed, Omaha NE, USA) was applied to the patient, and axial T2w fast spin echo images and diffusion-weighted images were acquired using scan parameters given in Table 1. The WPC was then removed, and the endorectal coil (Medrad eCoil, Bayer Medical Care, Indianola PA, USA) was inserted in usual fashion and the balloon inflated with 50–60 mL of air. The 32-channel pelvic phased array coil (GEM flex torso coil, GE Healthcare, Waukesha WI, USA) was positioned over the anterior lower abdomen and pelvis. Glucagon 1 mg IM was administered immediately following ERC insertion. Axial, coronal, and sagittal localizers were performed to assess ERC position, and adjustments were made if necessary. A standard diagnostic PI-RADS v2 prostate MRI protocol was then performed [10, 13]. As part of this protocol, axial T2w fast spin echo images were acquired using the ERC and PPA in unison. Two separate diffusion-weighted sequences were performed, one using the PPA coil only, and the other using the ERC only. The remaining sequences acquired as part of the standard diagnostic MRI were not used for the purposes of the study.

Qualitative image analysis

All images were reviewed on a diagnostic Picture Archiving and Communication System (PACS)

Table 1. Scan parameters (WPC, wearable pelvic coil; PPA, standard pelvic phased array coil; ERC, endorectal coil)

	T2w		DWI		
	WPC	ERC	WPC	PPA	ERC
Coil	WPC	ERC, PPA	WPC	PPA	ERC
b value (s/mm^2)	–	–	50, 1400	50, 1400	50, 1400
TR (ms)	4000–4394	4000	3300	3300	6000
TE (ms)	102–135	102	135	135	70–100
Slice thickness (mm)	3	3	4	4	4
Slice gap (mm)	0.5	0.5	0	0	0
Number of excitations	4	4	2, 16	2, 16	2, 12
Echo train length	13	13	–	–	–
Field of view (mm)	140–160	140	220	220	180
Acquisition matrix	256 × 256/224 × 256	288 × 192	96 × 96/120 × 50	96 × 96/120 × 50	96 × 96/96 × 128
Bandwidth (Hz)	20	20	166	166	166
Scan time	04:11–05:22	04:54	05:12–05:43	05:12–05:43	5:53–6:18

workstation (Centricity PACS RA1000; GE Healthcare, Barrington IL, USA). Qualitative image analysis was performed in consensus by two readers (ROD and RMD) with 4 years and 9 years experience respectively in prostate MRI. Wearable pelvic coil and endorectal coil T2w images were rated using six criteria, some of which have been employed in previous studies assessing prostate MR image quality [14, 15]. The T2w image criteria used were: definition of the posterior prostate gland border (PPGB; 1-5), the definition of zonal anatomy, i.e., the ability to distinguish the peripheral zone and transitional zone (ZA; 1–5), visualization of the neurovascular bundle (NVB; 1–4), visualization of the seminal vesicles (SV; 1–5), the severity of artifacts (SA; 1–4), and overall image quality (IQ; 1–5). Details of the scoring system are given in Table 2.

The three sets of DWI images were scored using five criteria, and some of these criteria were employed in a previous study assessing prostate DWI image quality [11]. The criteria used were margin demarcation defined by the ability to trace the prostate margin clearly (GD; 1–5), zonal anatomy defined by the ability to distinguish the peripheral zone and transitional zone clearly (ZA; 1–5), geometric distortion defined by distortion of the image due to field inhomogeneity using the T2w images as a reference (GD; 1–5), the severity of artifacts (SA; 1–4), and overall image quality (IQ; 1–5). In the cases of both T2w and DWI, the nature of any artifacts was recorded.

Quantitative image analysis

For the estimation of signal-to-noise ratios (SNRs) in the T2w and b1400 diffusion-weighted images, elliptical regions of interest (ROI) were placed over the peripheral zone of the prostate, the transitional zone of the prostate and the obturator internus muscle, avoiding any artifacts or focal lesions. The mean signal intensity was measured in the peripheral zone ROI and in the transitional zone ROI, and these two values were averaged to give a value for mean prostate gland signal. The standard deviation of the signal in the obturator internus muscle ROI was recorded to provide an estimation of image noise, and the SNR was calculated by dividing the mean prostate gland signal by the image noise [11, 16, 17].

Statistical analysis

All ordinal and continuous data are summarized as a mean ± standard deviation. The Wilcoxon matched-pairs signed rank test was used to test each variable for

Table 2. Image scoring system

Posterior prostate gland border visualization on T2w	Zonal anatomy distinction on T2w	Neurovascular bundle visualization on T2w
5. Well delineated	5. Excellent	4. Seen well on both sides
4. 75%–100% of margin clearly seen	4. Very good	3. Seen well on one side
3. 50%–75% of margin clearly seen	3. Good	2. Seen suboptimally on both sides
2. 25%–50% of margin clearly seen	2. Fair	1. Unreadable
1. < 25% of margin clearly seen	1. Poor	

Seminal vesicle visualization on T2w	Artifact severity on T2w	Overall T2w image quality
5. Margins and septations seen	4. Severe	5. Excellent
4. Margins seen, septations poorly seen	3. Moderate	4. Very good
3. Septations seen, margins poorly defined	2. Mild	3. Good
2. Poorly defined	1. None	2. Fair
1. Unreadable		1. Poor

Gland demarcation on DW	Zonal anatomy distinction on DWI	Geometric distortion on DWI
5. Excellent	5. Excellent	4. Severe
4. Very good	4. Very good	3. Moderate
3. Good	3. Good	2. Mild
2. Fair	2. Fair	1. None
1. Poor	1. Poor	

Artifact severity on DWI	Overall DWI image quality
4. Severe	5. Excellent
3. Moderate	4. Very good
2. Mild	3. Good
1. None	2. Fair
	1. Poor

Table 3. T2w image scores (WPC, wearable pelvic coil; ERC, endorectal coil)

	WPC	ERC	*p* value
Posterior border	4.44 ± 0.92	4.61 ± 0.70	0.563
Zonal anatomy	4.72 ± 0.57	4.78 ± 0.43	> 0.999
Neurovascular bundles	3.61 ± 0.78	4.39 ± 0.98	0.375
Seminal vesicles	4.40 ± 0.78	4.56 ± 0.61	0.500
Artifact severity	1.39 ± 0.70	2.01 ± 0.42	**0.003**
Overall image quality	3.83 ± 0.86	3.94 ± 0.42	0.796

Bold underlining value indicates statistical significance ($p < 0.05$)

statistical significance. A p value of < 0.05 was considered to indicate a statistically significant difference. Statistical analysis was performed using the GraphPad Prism software package (Version 7.0c, La Jolla, CA, USA).

Results

Qualitative T2w image analysis

The results of the qualitative T2w image analysis are given in Table 3. Artifact severity was greater in T2w images acquired with the endorectal coil compared with the wearable pelvic coil (ERC 2.01 ± 0.42 vs. WPC 1.39 ± 0.70, $p = 0.003$). Motion artifact in the phase encode direction emanating from the interface of the endorectal coil and rectal wall was seen in 17 of 18 ERC T2w sequences (Figs. 1 and 2). There was no statistically significant difference in overall image quality, posterior border definition, zonal anatomy distinction, neurovascular bundle visualization or seminal vesicle visualization.

Qualitative diffusion-weighted image analysis

The ability to clearly distinguish the peripheral zone and transitional zone on DWI was greater on images acquired with the endorectal coil compared with the wearable pelvic coil (ERC 4.28 ± 0.91 vs. WPC 3.72 ± 1.02, $p < 0.001$). ERC DWI images were also superior in clearly distinguishing the peripheral zone and transitional zone compared with the standard pelvic phased array coil (ERC 4.28 ± 0.91 vs. PPA 3.50 ± 0.92, $p = 0.018$) (Fig. 3). There was no significant difference in the abilities of the WPC and the PPA to distinguish zonal anatomy. There was no significant difference in the gland margin demarcation, geometric distortion, artifact severity and overall image quality between the WPC, PPA and ERC. Details of the qualitative DWI image analysis are given in Table 4.

Signal-to-noise ratio

The T2w signal-to-noise ratio was significantly higher in endorectal coil images than wearable pelvic coil images (ERC 38.32 ± 15.19 vs. WPC 16.57 ± 5.13, $p < 0.001$). Similarly, there were significantly higher signal-to-noise ratios comparing the endorectal coil DWI with the wearable pelvic coil DWI (ERC 81.49 ± 32.42 vs. WPC 19.83 ± 6.30, $p < 0.001$), and also comparing the endorectal coil DWI with the standard pelvic phased array coil DWI (ERC 81.49 ± 32. 42 vs. PPA 22.88 ± 13.62, $p < 0.001$). There was no significant difference comparing the DWI signal-to-noise ratio for the wearable pelvic coil and the standard pelvic phased array coil ($p = 0.865$).

Discussion

There is no clear consensus on the choice of imaging coil setup in mpMRI of the prostate. While ERC scanning at 3T is preferred at many institutions, the benefits associated with positioning the imaging coil in close proximity

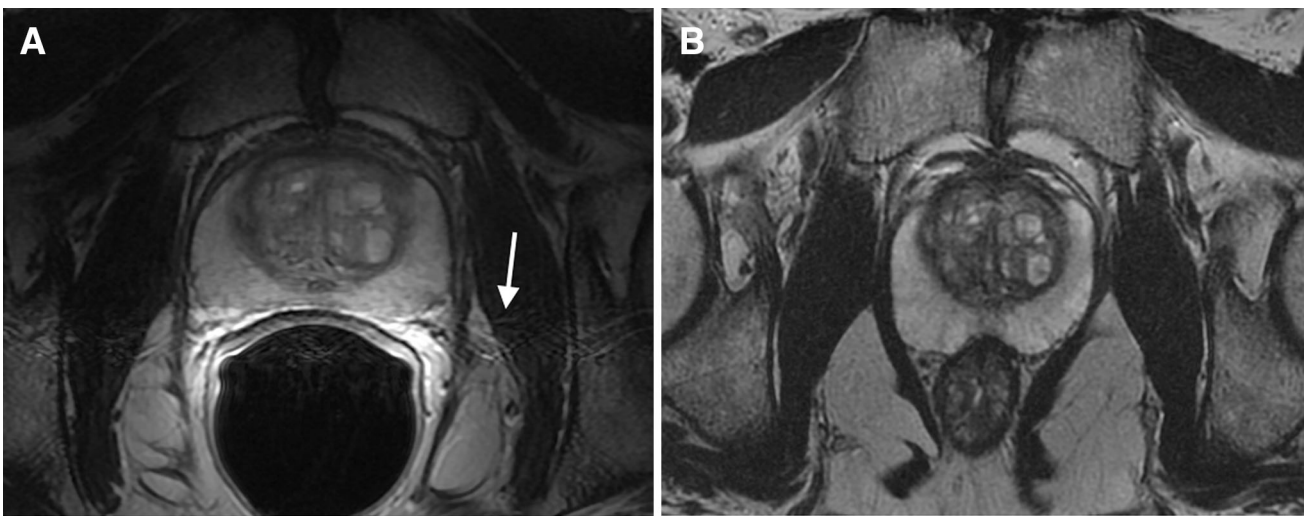

Fig. 1. T2w images from the same patient acquired with ERC (**A**) and WPC (**B**). Note the motion artifact on the ERC images emanating from the interface of the ERC and rectal wall (arrow).

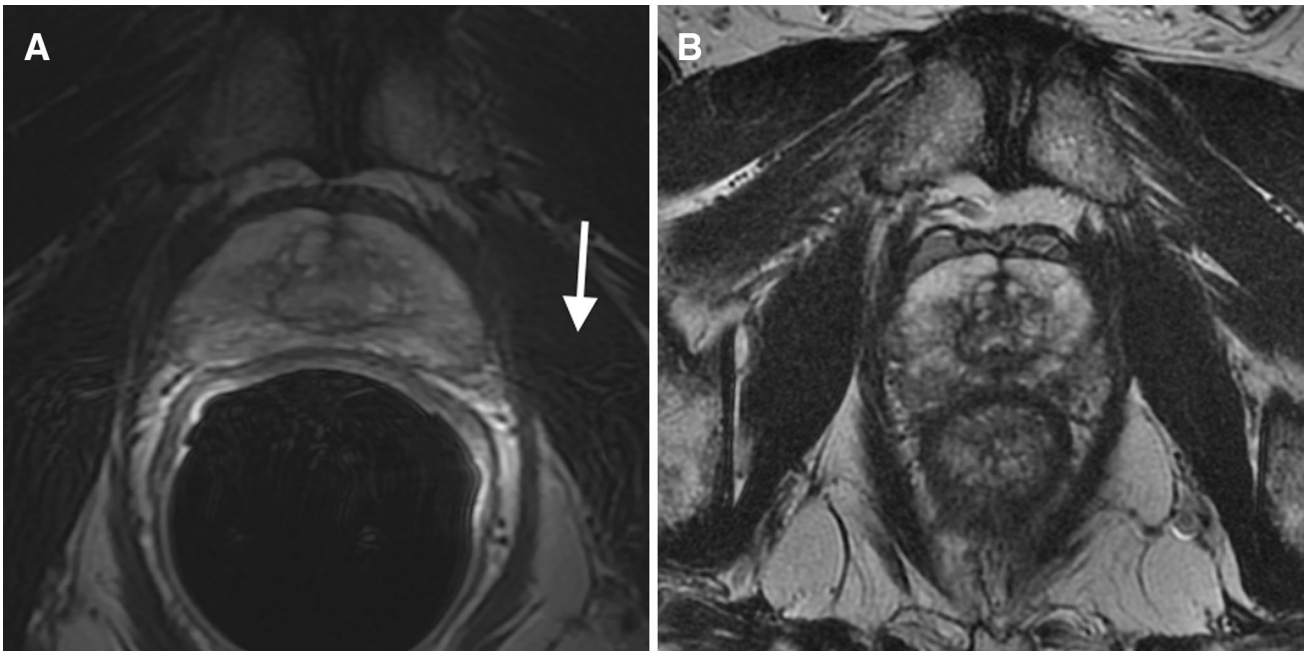

Fig. 2. T2w images acquired using ERC (**A**) and WPC (**B**). Motion artifact is again demonstrated on ERC images (arrow).

to the prostate gland must be balanced against potential penalties in the form of time, cost and patient discomfort. Indeed previous studies have been conducted demonstrating that ERC scanning is associated with increased patient discomfort compared with a standard PPA [11] and with a smaller colorectal endocoil [18]. With the expanding role of mpMRI of the prostate, these considerations are becoming more important.

The standard diagnostic pathway for prostate cancer until recently consisted of the performance of transrectal ultrasound guided biopsy (TRUS biopsy) in patients identified to be at risk by elevation of serum prostate specific antigen (PSA) or a suspicious digital rectal examination. Developing evidence supporting the use of mpMRI as part of a routine diagnostic pathway is leading to expansion of its utilization. Recently the PROMIS trial, a multicentre study examining the diagnostic accuracy of mpMRI and TRUS biopsy using template prostate mapping biopsy as a reference test, found mpMRI to have high sensitivity and negative predictive value for clinically significant prostate cancer, making it a potentially useful triage test by allowing some men to avoid unnecessary TRUS biopsy [9]. As the place of mpMRI solidifies, there are growing incentives for establishing techniques to acquire high-quality images without the need for ERC insertion.

The goal of ERC imaging is to acquire the maximum amount of signal from the small volume prostate gland at the highest possible resolution. A wearable pelvic imaging coil has been developed aiming to position the receive coil close to the prostate by enveloping the pelvis, allowing coil elements to pass between the upper thighs in close apposition to the perineum.

Previous studies have compared ERC and PPA imaging qualities across different field strengths [11, 12, 14, 19–25] however the literature directly comparing ERC and standard PPA imaging qualities at 3T is relatively sparse. Two studies comparing diagnostic performance at 3T found ERC imaging to be superior to non-ERC imaging for the detection of prostate cancer [12, 22]. However, it should be noted that in one of these two studies, both T2w and DWI using the ERC benefited from longer scan times than the PPA, and higher b values were used for the ERC DWI sequences [12]. Studies comparing ERC and PPA image quality at 3T have been somewhat conflicting. A study comparing T2w and DWI image quality at 3T found comparable results using an ERC or PPA for T2w, and superior DWI image quality for an ERC over PPA for one of two readers [11]. In this study, PPA DWI images profited from a higher number of excitations and longer scan times than ERC images, likely contributing in part to their good performance. In contrast to this, another study comparing T2w images at 3T found all image-quality characteristics apart from motion artifact to be better using an ERC than a PPA, although the ERC images benefited from smaller slice thickness and higher in-plane resolution [19].

In our study, we aimed to assess how a wearable pelvic coil compares with an endorectal coil in terms of T2w and DWI image quality. Our results found that the image quality for T2w using the wearable pelvic coil and endorectal coil are comparable, apart from lower artifact severity using the wearable pelvic coil. Motion artifact was prevalent on ERC T2w images, and was seen emanating in the phase encode direction from the interface of

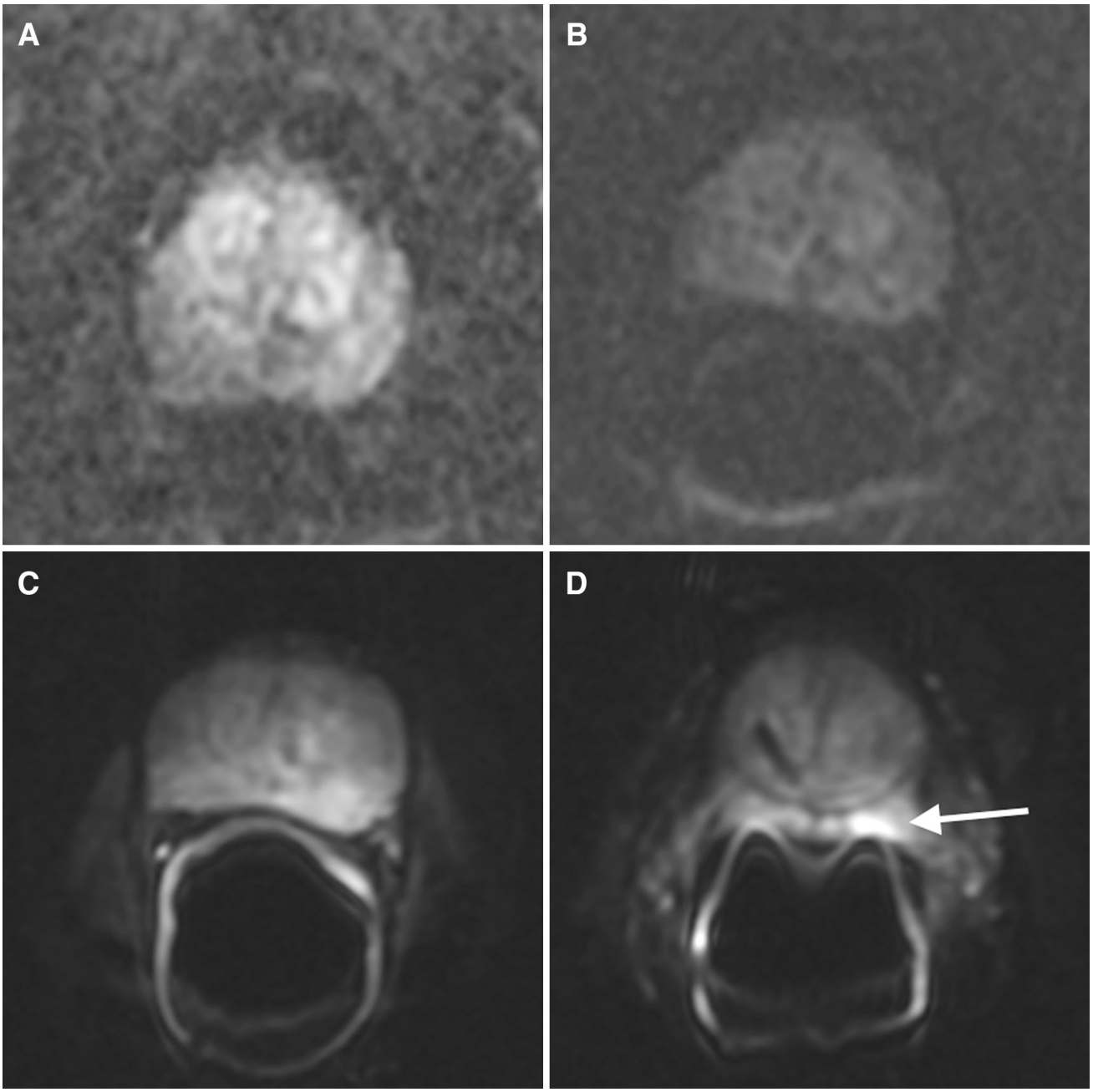

Fig. 3. DWI images from the same patient acquired using a wearable pelvic coil (**A**), standard pelvic phased array coil (**B**), and endorectal coil (**C**, **D**). Note the clearer delineation of the peripheral zone and transitional zone on endorectal coil images. There is high signal in the peripheral zone secondary to ERC related artifact (arrow).

Table 4. DWI image scores (p1 = WPC vs. PPA; p2 = WPC vs. ERC; p3 = PPA vs. ERC)

	WPC	PPA	ERC	p1	p2	p3
Gland margin demarcation	4.39 ± 0.61	4.28 ± 0.89	4.67 ± 0.59	0.781	0.188	0.016
Zonal anatomy	3.72 ± 1.02	3.50 ± 0.92	4.28 ± 0.91	0.219	**0.018**	< **0.001**
Geometric distortion	1.67 ± 0.91	1.72 ± 0.67	1.83 ± 0.62	> 0.999	0.637	0.689
Artifact severity	1.78 ± 0.88	2.00 ± 0.84	2.22 ± 0.65	0.463	0.097	0.289
Overall image quality	3.61 ± 0.61	3.61 ± 0.61	3.83 ± 0.51	> 0.999	0.344	0.289

Bold underlining values indicate statistical significance ($p < 0.05$)

the endorectal balloon and the anterior rectal wall in 17 of 18 patients.

For DWI image quality, the endorectal coil performed better than the wearable pelvic coil and also better than the standard pelvic phased array coil in distinguishing the peripheral zone from the transitional zone, but performance was comparable across the three coils using the criteria of gland margin demarcation, geometric distortion, artifact severity and overall image quality. There was no significant difference in any of the DWI image quality measures between the wearable pelvic coil and standard pelvic phased array coil. While high signal in the peripheral zone adjacent to the endorectal coil was a common finding on DWI images (being present in 15 of 18 ERC DWI sequences), geometric distortion was seen on many DWI sequences using the ERC, PPA and WPC, and overall there was no significant difference in artifact severity across the three coils.

The signal-to-noise ratio of T2w using the ERC was significantly higher than T2w using the WPC, and similarly the SNR of DWI was significantly higher for the ERC compared with both the WPC and PPA. There was no significant difference between the SNR of DWI images for the WPC and PPA. These findings support the perceived advantage of ERC imaging which provides a high SNR by placing the coil in as close proximity to the prostate gland as is possible. A similar difference in DWI SNR was seen in another study which found that the mean SNR using an ERC was 9.27 times higher in the peripheral zone and 5.52 times higher in the transitional zone compared with a phased array coil [25]. In contrast, another study by Barth et al. found a higher SNR for PPA DWI images compared with ERC images, and this was likely in part achieved due to the use of a longer scan time and higher numbers of excitations for PPA images [11]. The same study found a similar SNR for PPA and ERC T2w images, again likely accounted for by a higher number of excitations for the PPA images. Indeed in our study, ERC DWI images benefited from longer scan times than PPA or WPC, and the same numbers of excitations were used for both ERC and PPA T2w images, likely negating the advantages afforded for PPA imaging by the scan protocols of Barth et al. It could be suggested that in non-ERC scan protocols, longer scan times for WPC/PPA T2w and DWI images would be reasonable in the context of the time saved not inserting an ERC.

Our study had some limitations. First, we compared the quantitative and qualitative image quality of WPC and ERC imaging, but we did not assess diagnostic accuracy as not all patients proceeded to radical prostatectomy, and a reasonable reference standard was not available. Second, there was some variation in scan parameters across different patients which was a result of case-by-case attempts to optimize the image acquisition. Third, the ERC DWI sequences benefited from longer scan times compared with both WPC and PPA acquisitions, likely contributing in part to their higher SNR. Fourth, intramuscular glucagon was administered after the WPC imaging but before the ERC and PPA images were obtained, although in spite of this the artifact severity remained higher for ERC T2w images than for WPC T2w images. Fifth, 18 patients were suitable for inclusion in the study, and this sample size may have been insufficient to demonstrate more subtle differences in the qualitative assessment of image quality to a statistically significant degree. However, the numbers were sufficient to demonstrate statistically significant differences in T2w artifact severity and DWI zonal anatomy distinction as well as in the quantitative measurements of signal-to-noise ratios.

This study set out to compare the image quality using a wearable pelvic coil and an endorectal coil. The other main competing alternative to the wearable pelvic coil is imaging with a pelvic phased array coil alone. While an opportunistic qualitative and quantitative comparison of WPC and PPA DWI images was performed as part of this study due to the fact that both ERC and PPA DWI images were acquired as part of the standard scan protocol, T2w images were not compared. Further research will be required to more directly compare prostate imaging using a wearable pelvic coil and pelvic phased array coil.

In conclusion, wearable pelvic coil imaging provides comparable image quality to an endorectal coil, potentially reducing the need for an endorectal coil. Wearable pelvic coil imaging showed reduced T2w artifact severity and inferior DWI zonal anatomy distinction compared with an endorectal coil. Imaging with a wearable pelvic coil produces a lower signal-to-noise ratio than that with an endorectal coil.

Compliance with ethical standards

Funding ScanMed, the manufacturer of the PROCURE imaging coil system, provided one wearable pelvic coil to the Department of Radiology at the Brigham and Women's Hospital, and this was returned to ScanMed at the end of the study enrollment period. No further grant support was received.

Disclosures This study has been presented as an electronic poster at the European Congress of Radiology 2018 which has been published online on the ECR's EPOS system (https://dx.doi.org/10.1594/ecr2018/C-1171).

Conflict of interest Dr. Tempany declares no conflicts of interest relevant to the submitted work, and outside the submitted work reports grants from NIH, personal fees from Profound Medical and personal fees from Gilead Sciences. The other authors declare that they have no conflicts of interest.

Research involving Human Participants and/or Animals All procedures performed involving human participants were in accordance with the ethical standards of the institutional research committee, with the 1964 Helsinki declaration and with the Health Insurance Portability and Accountability Act.

Informed consent Written informed consent was obtained from all individual participants included in the study.

References

1. Fusco R, Sansone M, Petrillo M, et al. (2016) Multiparametric MRI for prostate cancer detection: preliminary results on quantitative analysis of dynamic contrast enhanced imaging, diffusion-weighted imaging and spectroscopy imaging. Magn Reson Imaging 34:839–845
2. Kurhanewicz J, Vigneron D, Carroll P, Coakley F (2008) Multiparametric magnetic resonance imaging in prostate cancer: present and future. Curr Opin Urol 18:71–77
3. Donati OF, Mazaheri Y, Afaq A, et al. (2013) Prostate cancer aggressiveness: assessment with whole-lesion histogram analysis of the apparent diffusion coefficient. Radiology 271:143–152
4. Donati OF, Afaq A, Vargas HA, et al. (2014) Prostate MRI: evaluating tumor volume and apparent diffusion coefficient as surrogate biomarkers for predicting tumor gleason score. Clin Cancer Res 20:3705–3711
5. Wu CJ, Wang Q, Li H, et al. (2015) DWI-associated entire-tumor histogram analysis for the differentiation of low-grade prostate cancer from intermediate–high-grade prostate cancer. Abdom Imaging 40:3214–3221
6. Costa DN, Bloch BN, Yao DF, et al. (2013) Diagnosis of relevant prostate cancer using supplementary cores from magnetic resonance imaging-prompted areas following multiple failed biopsies. Magn Reson Imaging 31:947–952
7. Cornud F, Brolis L, Delongchamps NB, et al. (2013) TRUS–MRI image registration: a paradigm shift in the diagnosis of significant prostate cancer. Abdom Imaging 38:1447–1463
8. Hoeks CMA, Somford DM, van Oort IM, et al. (2014) Value of 3-T multiparametric magnetic resonance imaging and magnetic resonance-guided biopsy for early risk restratification in active surveillance of low-risk prostate cancer: a prospective multicenter cohort study. Invest Radiol 49:165–172
9. Ahmed HU, El-Shater Bosaily A, Brown LC, et al. (2017) Diagnostic accuracy of multi-parametric MRI and TRUS biopsy in prostate cancer (PROMIS): a paired validating confirmatory study. Lancet 389:815–822
10. Weinreb JC, Barentsz JO, Choyke PL, et al. (2016) PI-RADS Prostate imaging—reporting and data system: 2015, Version 2. Eur Urol 69:16–40
11. Barth BK, Cornelius A, Nanz D, Eberli D, Donati OF (2016) Comparison of image quality and patient discomfort in prostate MRI: pelvic phased array coil vs. endorectal coil. Abdom Radiol 41:2218–2226
12. Turkbey B, Merino MJ, Gallardo EC, et al. (2014) Comparison of endorectal coil and nonendorectal coil T2 W and diffusion-weighted MRI at 3 Tesla for localizing prostate cancer: correlation with whole-mount histopathology. J Magn Reson Imaging 39:1443–1448
13. Barentsz JO, Richenberg J, Clements R, et al. (2012) ESUR prostate MR guidelines 2012. Eur Radiol 22:746–757
14. Shah ZK, Elias SN, Baza R, et al. (2015) Performance comparison of 1.5-T endorectal coil MRI with 3.0-T nonendorectal coil MRI in patients with prostate cancer. Acad Radiol 22:467–474
15. Sosna J, Pedrosa I, Dewolf WC, et al. (2004) MR imaging of the prostate at 3 Tesla: comparison of an external phased-array coil to imaging with an endorectal coil at 1.5 Tesla. Acad Radiol 11:857–862
16. Heverhagen JT (2007) Noise measurement and estimation in MR imaging experiments. Radiology 245:638–639
17. Kaufman L, Kramer DM, Crooks LE, Ortendahl DA (1989) Measuring signal-to-noise ratios in MR imaging. Radiology 173:265–267
18. Powell DK, Kodsi KL, Levin G, et al. (2014) Comparison of comfort and image quality with two endorectal coils in MRI of the prostate. J Magn Reson Imaging 39:419–426
19. Heijmink SW, Fütterer JJ, Hambrock T, et al. (2007) Prostate cancer: body-array versus endorectal coil MR imaging at 3 T–comparison of image quality, localization, and staging performance. Radiology 244:184–195
20. Park BK, Kim B, Kim CK, Lee HM, Kwon GY (2007) Comparison of phased-array 3.0-T and endorectal 1.5-T magnetic resonance imaging in the evaluation of local staging accuracy for prostate cancer. J Comput Assist Tomogr 31:534–538
21. Torricelli P, Cinquantini F, Ligabue G, et al. (2006) Comparative evaluation between external phased array coil at 3T and endorectal coil at 1.5T: preliminary results. J Comput Assist Tomogr 30:355
22. Costa DN, Yuan Q, Xi Y, Rofsky NM, et al. (2016) Comparison of prostate cancer detection at 3-T MRI with and without an endorectal coil: a prospective, paired-patient study. Urol Oncol 34:255.e7–255.e13. https://doi.org/10.1016/j.urolonc.2016.02.009
23. Fütterer JJ, Engelbrecht MR, Jager GJ, et al. (2007) Prostate cancer: comparison of local staging accuracy of pelvic phased-array coil alone versus integrated endorectal-pelvic phased-array coils. Local staging accuracy of prostate cancer using endorectal coil MR imaging. Eur Radiol 17:1055–1065
24. Hricak H, White S, Vigneron D, et al. (1994) Carcinoma of the prostate gland: MR imaging with pelvic phased-array coils versus integrated endorectal–pelvic phased-array coils. Radiology 193:703–709
25. Mazaheri Y, Vargas HA, Nyman G, et al. (2013) Diffusion-weighted MRI of the prostate at 3.0 T: comparison of endorectal coil (ERC) MRI and phased-array coil (PAC) MRI-The impact of SNR on ADC measurement. Eur J Radiol 82:e515–e520. https://doi.org/10.1016/j.ejrad.2013.04.041